A Letters Journal Exploring the Frontiers of Physics

OFFPRINT

The branch with the furthest reach

Z. Wei, S. Mandre and L. Mahadevan

EPL, **97** (2012) 14005

A Letters Journal Exploring the Frontiers of Physics

January 2012

EPL, **97** (2012) 14005
doi: 10.1209/0295-5075/97/14005

www.epljournal.org

The branch with the furthest reach

Z. Wei, S. Mandre and L. Mahadevan[(a)]

School of Engineering and Applied Sciences, and Department of Physics, Harvard University Cambridge, MA 02138, USA

received 16 June 2011; accepted in final form 17 November 2011
published online 3 January 2012

PACS 46.70.De – Beams, plates, and shells
PACS 46.15.Cc – Variational and optimizational methods
PACS 02.30.Yy – Control theory

Abstract – How should a given amount of material be moulded into a cantilevered beam clamped at one end, so that it will have the furthest horizontal reach? Here, we formulate and solve this variational problem for the optimal variation of the cross-section area of a heavy cantilevered beam with a given volume V, Young's modulus E, and density ρ, subject to gravity g. We find that the cross-sectional area should vary according a universal profile that is independent of material parameters, with both the length and maximum reach-out distance of the branch that scale as $(EV/\rho g)^{1/4}$, with a universal self-similar shape at the tip with the area of cross-section $a \sim s^3$, s being the distance from the tip, consistent with earlier observations of tree branches, but with a different local interpretation than given before. A simple experimental realization of our optimal beam shows that our result compares favorably with that of our observations. Our results for the optimal design of slender structures with the longest reach are valid for cross-sections of arbitrary shape that can be solid or hollow and thus relevant for a range of natural and engineered systems.

Structural optimization for stiffness and strength has a venerable history in biology [1] and technology [5], in the context of both natural and man-made examples such as trabecular bone [2], tree height [3], soft architectures [4] and engineering [6,7], with simultaneous developments in mathematical optimization [5]. A classical example of such a question is that of designing a column with a cross-section that maximizes its resistance to buckling under compression [8] or under its own weight, as in a tree [9], and has inspired the analysis of many related problems [10,11], all of which focus on analyzing the optimization of columns to buckling. Here we analyze a complementary problem, that of maximizing the reach of a cantilevered beam that projects out horizontally from a support, much as a tree branch would. Of course, the shape of tree branches is likely a consequence of multiple considerations including structural support, mass transport, light interception for photosynthesis etc. [12]. While multiple mechanisms like branching, variation of leaf shape, etc. all play a role, one important function of a branch is to reach further away from the main trunk to better intercept sunlight. However, in the presence of gravity, branches droop: the droop is small for short stubby branches which are almost horizontal, but very pronounced for long slender branches. This raises a natural question: given a certain volume of material, what is the optimal variation of the cross-sectional shape of a branch that has the maximum horizontal reach? Although the direct connection to the shape of tree branches will require a consideration of an objective function that depends dynamically on multiple variables, here we take a first step and study the structural optimization problem of farthest reach by redistributing the mass of the branch along its length. This problem is also of intrinsic interest as it is one of the simplest non-linear problems in structural optimization that combines geometry and mechanics in a non-trivial setting: almost trivial to state, yet with many subtleties as we shall see. Indeed, even at a minimal level, given that there are two length scales in the problem: i) an extrinsic one associated with the volume of the material and ii) an intrinsic one associated with the competition between elasticity and gravity, it is *a priori* not obvious which combination of these two lengths does the maximal reach scale with. In particular, since we do not know *a priori* if the branch is weakly or strongly deformed, we cannot be sure how to combine these two scales. Here we formulate and solve this optimization problem using a combined analytical-numerical method and find that the solution has a universal solution that is independent of material parameters for self-similar

[(a)]E-mail: lm@seas.harvard.edu

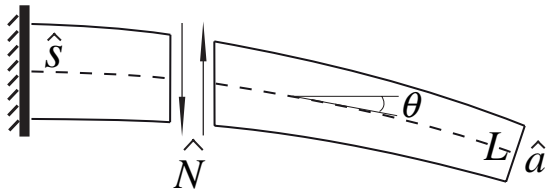

Fig. 1: A cantilevered branch showing the geometry and notation: $\hat{s}$ is the arc length, $\hat{s} \in (0, L)$, $\hat{N}$ is the vertical shear force, $\hat{a}$ is the cross-sectional area profile, θ is the angle of the center line tangent with the horizontal direction.

cross-sections. Furthermore, we find that the tip of this optimal beam points vertically downwards with a scale-invariant singular behavior at its sharp tip. Our results are consistent with available data on tree branch shapes but with a fundamentally different interpretation.

For simplicity, we will assume that the branch is made of an isotropic, homogeneous linearly elastic material with a density ρ, Young's modulus E, volume V subject to gravity g. We will assume that the dominant mode of deflection of the branch is via inextensional bending, consistent with its slender aspect ratio. If the angle of the center line tangent with the horizontal direction is $\theta(\hat{s})$, where $\hat{s}$ is the arc-length coordinate measured from the clamped support, the horizontal reach of the branch is

$$X(L) = \int_0^L \cos\theta(\hat{s})\,\mathrm{d}\hat{s}, \tag{1}$$

where L is the (as yet unknown) length of the middle (neutral) axis of the branch (see fig. 1). Torque and force balance on the beam yield the equations [13],

$$\begin{aligned} \left(cE\hat{a}^2(\hat{s})\theta_{\hat{s}}(\hat{s})\right)_{\hat{s}} + \hat{N}(\hat{s})\cos\theta(\hat{s}) = 0, \\ \hat{N}_{\hat{s}}(\hat{s}) + \rho g\hat{a}(\hat{s}) = 0; \end{aligned} \tag{2}$$

where $cE\hat{a}^2$ is the bending stiffness of the branch of unknown cross-sectional area profile $\hat{a}(\hat{s})$, which is not restricted to any particular shape, but can be hollow, solid, polygonal or smooth etc. Our results of the shape of the optimal beam are not limited to solid cross-sections or indeed circular cross-sections, since it is only the area and the second moment of the cross-section that enters the analysis. Here we have chosen not to also let the cross-section itself be a variable since there are highly singular non-convex cross-sections that can arise as solutions even in the simpler linear problem of maximizing the buckling load [8,10]. Instead we choose a few representative cross-sections starting with the simplest —a solid circular cross-section. The dimensionless parameter c characterizes the geometry of the cross-section; for a circular cross-section, $c = 1/(4\pi)$. Here $\hat{N}$ is the vertical shear force, and $(\cdot)_{\hat{s}} \equiv \mathrm{d}(\cdot)/\mathrm{d}\hat{s}$ (see fig. 1). Since the weight of the branch has to be supported by the vertical force at the clamped end, we must further have

$$\hat{N}(0) = \rho g V. \tag{3}$$

In addition, the boundary conditions associated with a horizontally clamped base and a free tip are given by

$$\theta(0) = 0, \quad \hat{N}(L) = 0, \quad (\hat{a}^2\hat{\theta}_{\hat{s}})\big|_L = 0. \tag{4}$$

Then our nested optimization problem corresponds to optimizing the reach of the branch subject to a given volume and the equations of equilibrium that are treated as constraints. Thus, we must determine $\hat{a}(\hat{s})$ by maximizing the reach (1) with the equations of equilibria (2) as constraints, so that the following Lagrangian suggests itself:

$$\begin{aligned} \Omega(\hat{a}, L, \theta, \hat{N}; \hat{\beta}, \hat{\eta}) = \int_0^L \cos\theta\,\mathrm{d}\hat{s} + \int_0^L \hat{\eta}(\hat{s})(\rho g\hat{a} + \hat{N}_{\hat{s}})\,\mathrm{d}\hat{s} \\ + \int_0^L \hat{\beta}(\hat{s})[cE(\hat{a}^2\theta_{\hat{s}})_{\hat{s}} + \hat{N}\cos\theta]\,\mathrm{d}\hat{s}, \end{aligned} \tag{5}$$

where $\hat{\beta}$ and $\hat{\eta}$ are Lagrange multipliers. It is important to note here that although the equations of equilibrium can themselves be derived from an elastic energy functional, that functional does not enter into the formulation of the optimal reach problem, even though the final solution will obviously also minimize that energy (as it satisfies the equations of equilibrium). Upon using the scaled variables $\hat{s} = L(1-s)$, $\hat{a} = (V/L)a$, $\hat{N} = (\rho g V)N$, $\hat{\beta} = 1/(\rho g V)\beta$, $\hat{\eta} = L/(\rho g V)\eta$, and taking variations of the functional (5) with respect to all the independent variables, respectively, we get the Euler-Lagrange equations

$$\begin{aligned} (a^2\theta_s)_s + \chi N\cos\theta = 0, \\ N_s - a = 0, \\ (a^2\beta_s)_s - \chi(1+\beta N)\sin\theta = 0, \\ \eta_s + \beta\cos\theta = 0, \\ \chi\eta - 2a\beta_s\theta_s = 0, \end{aligned} \tag{6}$$

where the dimensionless parameter $\chi = \rho g L^4/(cEV)$ is an (unknown) eigenvalue of the system. The problem as posed is now independent of any material parameters, and allows us to see that the characteristic length of our branch $L \sim (EV/\rho g)^{1/4}$ is a combination of the intrinsic elastic-gravity length $E/\rho g$ and the extrinsic length $V^{1/3}$.

With $s = 0$ being the free tip, $s = 1$ now corresponds to the clamped end, so that the natural boundary conditions(BCs) associated with variation of the functional (5) along with (3), (4) read

$$\begin{aligned} (a\beta\theta_s\delta a)\big|_0^1 &= 0, & (-a^2\beta_s\delta\theta + a^2\beta\delta\theta_s)\big|_0^1 = 0, \\ (\eta\delta N)\big|_0^1 &= 0, & N(0) = 0, \quad N(1) = 1, \\ \cos\theta(0) &= 0, & \theta(1) = 0, \quad (a^2\theta_s)\big|_0 = 0. \end{aligned} \tag{7}$$

We see immediately that the condition on the angle of the center line of the beam at the tip $\cos\theta(0) = 0$ in (7) implies that $\theta \to \pi/2$, *i.e.* the tip points vertically downwards.

Intuitively, if the tip does not do so, by adding more material there, it is possible to extend the beam a little further in the horizontal direction.

As noted previously, there are two global natural scales in the problem, an intrinsic one associate with the balance between gravity and elasticity, and an extrinsic one associated with a given volume. However, near the tip neither of these can play any role locally and we expect a scale-invariant asymptotic solution of (6) near the tip. Furthermore, the asymptotic behavior at the tip is also expected to be singular, because both the branch weight driving bending and the bending stiffness resisting it are functions of the cross-sectional area which vanishes as we approach the vertically oriented tip. In light of this, we may simplify (6) in the neighborhood of the free tip $\theta = \pi/2 - \alpha$, where $\alpha \ll 1$, by expanding terms in powers of α, which then yields, at leading order,

$$(a^2\alpha_s)_s - \chi N\alpha = 0, \tag{8}$$

$$N_s - a = 0, \tag{9}$$

$$(a^2\beta_s)_s - \chi(1+\beta N) = 0, \tag{10}$$

$$\eta_s + \beta\alpha = 0, \tag{11}$$

$$\chi\eta + 2a\beta_s\alpha_s = 0 \tag{12}$$

with the tip BCs from (7) that read

$$(a\beta\alpha_s\delta a)\big|_0 = 0, \tag{13}$$

$$(a^2\beta_s)|_0 = 0, \quad (a^2\alpha_s)\big|_0 = 0, \quad N(0) = 0, \tag{14}$$

where we have retained (13) entirely instead of $(a\beta\theta_s)|_0 = 0$ for reasons that will be clarified later. Looking for a power-law form of the cross-section profile $a = a_0\, s^p$, and noting that $N(0) = 0$, yields $N = a_0 s^{p+1}/(p+1)$. On substituting these expressions into (8), and balancing the powers and coefficients, respectively, we obtain $p = 3$ and

$$\alpha = \alpha_{01}s^{n_1} + \alpha_{02}s^{n_2}, \quad n_{1,2} = \frac{-5 \pm \sqrt{25 + \chi/a_0}}{2}, \tag{15}$$

where $\alpha_{01,02}$ are integration constants to be determined. As both $\chi, a_0 > 0$, imposing the BC $(a^2\alpha_s)|_0 = 0$, implies that the negative power $n_2 < -5$ must be discarded. Since the homogenous part of (10) has the same structure as (8), it follows that

$$\beta = \beta_0 s^{n_1} + \beta_p, \quad \beta_p = -\frac{4\chi}{a_0(16a_0+\chi)}s^{-4}, \tag{16}$$

where β_0 is an integration constant. Then, on inserting a, N, α and β into (11) and (12) yields two different expressions for the Lagrange multiplier η

$$\eta = \alpha_0\left(\frac{4\chi s^{n_1-3}}{a_0(n_1-3)(16a_0+\chi)} - \frac{\beta_0\, s^{2n_1+1}}{2n_1+1}\right) + \eta_0, \tag{17}$$

$$\eta = 2n_1\alpha_0\left(-\frac{16\, s^{n_1-3}}{16a_0+\chi} - \frac{a_0 n_1\beta_0\, s^{2n_1+1}}{\chi}\right). \tag{18}$$

Equating (17) and (18) implies that the integration constant $\eta_0 = 0$. Since s^{n_1-3} term is dominant as $s \to 0$ (near the tip), and n_1 is given by (15), this implies that $\beta_0 = 0$ and yields $a_0 = 9\chi/64$ and $n_1 = 1/3$. Thus, the only self-consistent power law solutions in the vicinity of the tip are

$$\begin{aligned} &a = \frac{9\chi}{64}s^3, \quad N = \frac{9\chi}{256}s^4, \quad \alpha = \alpha_0 s^{\frac{1}{3}}, \\ &\beta = -\frac{1024}{117\chi}s^{-4}, \quad \eta = -\frac{128\alpha_0}{39\chi}s^{-\frac{8}{3}}. \end{aligned} \tag{19}$$

Although we have used the BCs (14), we note that $(a\beta\alpha_s)|_0 \sim s^{-5/3}$ in fact blows up, *i.e.* (13) is not satisfied. However, an appropriate transformation of the area $a = b^x$ followed by the use of b instead of a as the independent variable in the functional (5), changes neither (8)–(12) nor the power law relations (19), but the BC (13) becomes

$$s^{3(x-1)/x}s^{-4}s^{-1}s^{1/3} = 0 \quad \text{as} \quad s \to 0. \tag{20}$$

Clearly, any $x > 9/4$ will satisfy (20), *i.e.* we must choose our solutions from a function space carefully to ensure differentiability. When the vanishing of the first variation of a functional is used as the criterion to find the extrema, the first variation must be well defined and non-divergent. As seen from the divergence of $(a\beta\alpha_s)_0$, the first variation of our functional with respect to the cross-sectional area $a(s)$ is divergent indicating a singular dependence of our functional in (6) on $a(s)$. Formally, this singularity is treated by simply using b instead of a as the independent function.

Knowing the asymptotic self-similar singular solution of the linearized problem near the tip, we can peel it away to determine the remaining non-singular non-linear solution, inspired by a similar procedure recently used to solve singular linear eigenvalue problems [11]. Writing the complete solution as the product of similarity solution (19) and a new set of variables $\{\bar{a},\ \bar{N},\ \bar{\alpha},\ \bar{\beta},\ \bar{\eta}\}$,

$$\begin{aligned} &a = \frac{9\chi}{64}s^3\bar{a}, \quad N = \frac{9\chi}{256}s^4\bar{N}, \quad \alpha = \alpha_0 s^{\frac{1}{3}}\bar{\alpha}, \\ &\beta = -\frac{1024}{117\chi}s^{-4}\bar{\beta}, \quad \eta = -\frac{128\alpha_0}{39\chi}s^{-\frac{8}{3}}\bar{\eta}, \end{aligned} \tag{21}$$

we require that as we approach the tip, $\{\bar{a},\ \bar{N},\ \bar{\alpha},\ \bar{\beta},\ \bar{\eta}\} \to \{1,\ 1,\ 1,\ 1,\ 1\}$ as $s \to 0$. Away from the tip, on substituting (21) and $\theta = \pi/2 - \alpha$ into (6), and using a transformed spatial variable $t = -\ln s$ (see footnote [1]) leads to an algebraically complex, but numerically tractable

[1] By using t as the independent variable, we get an autonomous linear system for which the normal modes are easily found.

7th-order system of equations for the new variables

$$\begin{aligned}
\bar{a}' &= -\frac{16e^{t/3}\sin(e^{-t/3}\alpha_0\bar{\alpha})(2\bar{a}\bar{\beta}+\bar{N}(4\bar{\beta}+\bar{\beta}'))}{9\alpha_0\bar{a}(\bar{\alpha}-3\bar{\alpha}')(4\bar{\beta}+\bar{\beta}')} \\
&\quad +\frac{4\cos(e^{-t/3}\alpha_0\bar{\alpha})(4\bar{N}\bar{\beta}-13)}{27\bar{a}(4\bar{\beta}+\bar{\beta}')}+3\bar{a}, \\
\bar{N}' &= 4(\bar{N}-\bar{a}), \\
\bar{\alpha}'' &= \frac{16e^{t/3}\bar{N}\sin(e^{-t/3}\alpha_0\bar{\alpha})}{9\alpha_0\bar{a}^2}+\frac{2\bar{a}'(\bar{\alpha}-3\bar{\alpha}')}{3\bar{a}} \\
&\quad +\frac{51\bar{\alpha}'-16\bar{\alpha}}{9}, \\
\bar{\beta}'' &= \frac{4\cos(e^{-t/3}\alpha_0\bar{\alpha})(4\bar{N}\bar{\beta}-13)}{9\bar{a}^2}-\frac{\bar{a}'(8\bar{\beta}+2\bar{\beta}')}{\bar{a}} \\
&\quad +4\bar{\beta}-3\bar{\beta}', \\
\bar{\eta}' &= \frac{8}{3}\left(-\bar{\eta}+\frac{e^{t/3}\bar{N}\sin(e^{-t/3}\alpha_0\bar{\alpha})}{\alpha_0}\right),
\end{aligned} \tag{22}$$

where $(\cdot)' \equiv \mathrm{d}(\cdot)/\mathrm{d}t$ (with $t=0$ corresponds to the clamped base), along with the BCs (7) there that now read

$$\bar{\beta}(0)=0, \quad \bar{\alpha}(0)-\frac{\pi}{2\alpha_0}=0, \quad \bar{N}(0)=\frac{256}{9\chi}. \tag{23}$$

To solve the above non-linear non-singular equations away from the tip, we first determine a stable characteristic direction of the non-singular system by inserting (19) into (8)–(12), and perturb about the homogeneous BCs so that $\bar{a}=1+\delta\bar{a}$, $\bar{N}=1+\delta\bar{N}$, $\bar{\alpha}=1+\delta\bar{\alpha}$, $\bar{\beta}=1+\delta\bar{\beta}$, $\bar{\eta}=1+\delta\bar{\eta}$, and derive a linear set of ODEs that reads

$$\begin{aligned}
32\delta\bar{a}-16\delta\bar{N}-6\delta\bar{a}'-51\delta\bar{\alpha}'+9\delta\bar{\alpha}''&=0, \\
-4\delta\bar{a}+4\delta\bar{N}-\delta\bar{N}'&=0, \\
72\delta\bar{a}+16\delta\bar{N}+52\delta\bar{\beta}-72\delta\bar{a}'-27\delta\bar{\beta}'-9\delta\bar{\beta}&=0, \\
8\delta\bar{\alpha}+8\delta\bar{\beta}-8\delta\bar{\eta}-3\delta\bar{\eta}'&=0, \\
-4\delta\bar{a}-4\delta\bar{\alpha}-4\delta\bar{\beta}+4\delta\bar{\eta}+12\delta\bar{\alpha}'-\delta\bar{\beta}'&=0.
\end{aligned} \tag{24}$$

Substitution of the normal mode form,

$$\begin{aligned}
&\delta\bar{a}=\delta\bar{a}_0e^{qt}, \quad \delta\bar{N}=\delta\bar{N}_0e^{qt}, \quad \delta\bar{\alpha}=\delta\bar{\alpha}_0e^{qt}, \\
&\delta\bar{\beta}=\delta\bar{\beta}_0e^{qt}, \quad \delta\bar{\eta}=\delta\bar{\eta}_0e^{qt},
\end{aligned} \tag{25}$$

into (24) gives us 5 equations about the coefficients $\{\delta\bar{a}_0,\ \delta\bar{N}_0,\ \delta\bar{\alpha}_0,\ \delta\bar{\beta}_0,\ \delta\bar{\eta}_0\}$. For non-trivial solutions to exist, the Jacobian has to vanish, resulting in a 6th-order polynomial equation for the eigenvalue q whose solutions are

$$\begin{aligned}
q_1 &= 0, \quad q_2=\frac{1}{3}, \quad q_3=1, \quad q_4=\frac{4}{3}, \\
q_5 &= \frac{2}{3}(1-\sqrt{105}), \quad q_6=\frac{2}{3}(1+\sqrt{105}).
\end{aligned}$$

Of these, the only viable mode corresponds to that associated with the solution $q_5<0$, since as we approach the tip, $t\to\infty$ and $\lim_{t\to\infty}\exp(q_5t)\to 0$, as required. The corresponding stable eigenvector is given by

$$\begin{pmatrix}\delta\bar{a}_0\\ \delta\bar{N}_0\\ \delta\bar{\alpha}_0\\ \delta\bar{\beta}_0\\ \delta\bar{\eta}_0\end{pmatrix}=\begin{pmatrix}3\left(4575-467\sqrt{105}\right)/5048\\ 5\left(-327+28\sqrt{105}\right)/631\\ \left(151-11\sqrt{105}\right)/1262\\ 3\left(951-203\sqrt{105}\right)/2524\\ 1\end{pmatrix}. \tag{26}$$

Thus the asymptotic BCs for the non-linear system that characterizes the non-singular part of the solution $\{\bar{a},\ \bar{N},\ \bar{\alpha},\ \bar{\beta},\ \bar{\eta}\}$ in the vicinity of the free tip is given by

$$\begin{aligned}
&\{\bar{a}\ \bar{N}\ \bar{\alpha}\ \bar{\alpha}'\ \bar{\beta}\ \bar{\beta}'\ \bar{\eta}\}=\{1\ 1\ 1\ 0\ 1\ 0\ 1\} \\
&+\Delta\{\delta\bar{a}_0\ \delta\bar{N}_0\ \delta\bar{\alpha}_0\ q_5\delta\bar{\alpha}_0\ \delta\bar{\beta}_0\ q_5\delta\bar{\beta}_0\ \delta\bar{\eta}_0\},
\end{aligned} \tag{27}$$

where Δ is an unknown perturbation magnitude at a fixed position t close to the tip.

Finally, using (27) as an initial condition at a short distance away from the tip in terms of the new variables in (21) we can now solve the non-linear problem (6), (7) numerically using a shooting method to satisfy the conditions $\bar{\beta}(0)=0$, $\bar{\alpha}(0)=\pi/(2\alpha_0)$. This allows us to determine the unknown constants α_0 and Δ, as well as the shape of the scaled branch cross-section $a(s)$ and droop $\theta(s)$. This calculation also yields the unknown eigenvalue $\chi=\rho gL^4/(cEV)\approx 49.01$, and the dimensionless reach-out distance $\int_0^1\cos\theta\,\mathrm{d}s\approx 0.84$. Then the dimensional length of the neutral axis of the optimal branch $L\approx 1.41(EV/\rho g)^{1/4}$, and the maximum reach-out distance in the horizontal direction $X\approx 1.18(EV/\rho g)^{1/4}$ with a relatively weak dependence on the volume and elastic modulus of the material. Since material and geometrical constants enter this problem only via χ, the scaled geometrical quantities characterizing the shape of the branch are all universal functions. In fig. 2(a), we show the cross-section $a(s)$, in fig. 2(b), we show the angle θ that the center line makes with the horizontal, in fig. 2(c), we show the bending moment $a^2\theta_s$ and finally, in fig. 2(d) we show the shape of the beam (for the case of an assumed circular cross-section).

To test our predictions qualitatively, we used a 3D printer (Objet Connex) to manufacture a polymeric (TangoBlack) optimal beam with a circular cross-section using our calculated optimal shape (fig. 3(b)). In fig. 3(c), we show the theoretical and experimental shapes for the parameter values $V=20\,\mathrm{cm}^3$, $E=0.63\,\mathrm{MPa}$, $\rho=1150\,\mathrm{kg/m}^3$. The small discrepancy between the theoretical longest reach 0.215 m and the measured reach of 0.211 m is likely due to the expansion of the polymer as it cures, which results in asymmetric cross-section, inhomogeneous density and Young's modulus, and residual strains.

To contrast our true optimal solution with those associated with a prescribed cross-sectional profile, we consider the simple cases of a uniform cylindrical column and a right-circular cone. For cylinders,

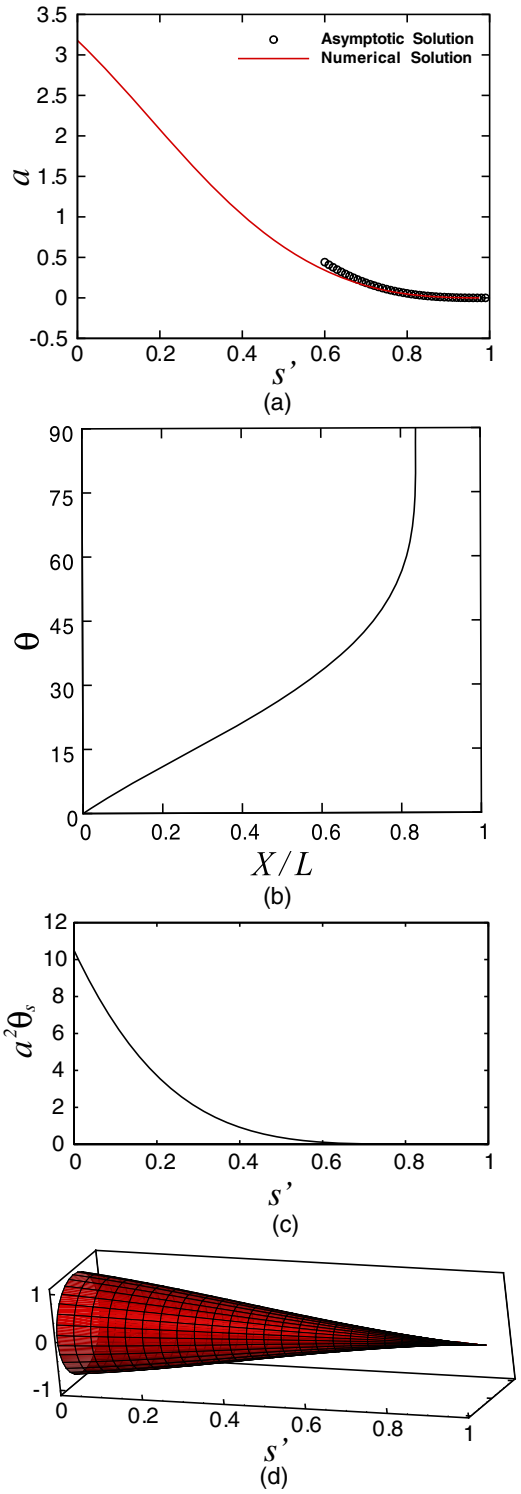

Fig. 2: (Colour on-line) (a) The dimensionless optimal cross-sectional area a as a function of arc length s' ($s' = 1 - s$), determined by solving (21), (6). Near the tip ($s = 0$), $a \sim s^3$ consistent with (19). (b) Under the influence of gravity, the optimal branch is vertical at the tip, but deviates rapidly from this as one moves towards the base. (c) The bending moment $a^2\theta_s$ increases monotonically from the tip towards the base, where it has its maximum value. (d) A 3-dimensional depiction of the optimal cross-section for the case when the cross-section is a circular disc.

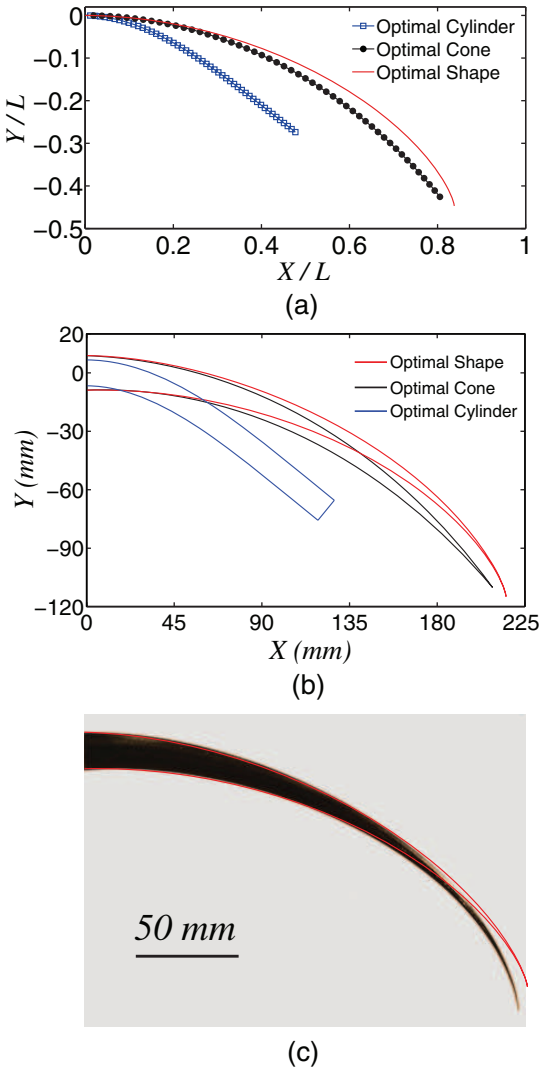

Fig. 3: (Colour on-line) (a) Scaled deflection of the neutral axes of the optimal branch with the furthest reach, compared to the optimal cone and optimal cylinder. All scaled shapes are universal (see text); the apparently shorter reach of the optimal branch is a consequence of the larger value of L for this solution. (b) Comparison of the droop of the optimal branch with the longest reach and that of an optimal cone and and an optimal cylinder for a given volume $V = 20\,\mathrm{cm}^3$, Young's modulus $E = 0.63\,\mathrm{MPa}$ and density $\rho = 1150\,\mathrm{kg/m}^3$. (c) Comparison of the drooping shape of a branch made of a polymer with our theoretical prediction; the small difference between the two is due to the expansion of the polymer on curing.

we let the scaled area of cross-section area $a = 1$ and for cones, we let $a = 3(s+\epsilon)^2/(1+3\epsilon+3\epsilon^2)$, where $\epsilon = 10^{-5} \ll 1$, a cutoff to prevent singular behavior at the tip. Then, maximizing $L\int_1^0 \cos\theta\,\mathrm{d}s$ subject to the constraint $(a^2\theta_s)_s + \chi(\int_0^s a\,\mathrm{d}s)\cos\theta = 0$ yields $\chi = 4.886$ for the optimal cylinder, so that $L_{cyl} \approx 0.79(EV/\rho g)^{1/4}$, and $X_{cyl} \approx 0.67(EV/\rho g)^{1/4}$, while $\chi = 39.90$ for the optimal cone, so that $L_{cone} \approx 1.33(EV/\rho g)^{1/4}$ and $X_{cone} \approx 1.14(EV/\rho g)^{1/4}$. In fig. 3(a), we compare the

center lines of the scaled drooping optimal cylinder and the optimal cone with the optimal shape, and find that the optimal branch reaches out 43% further than the optimal cylinder, but only 3% further than the optimal cone of the same volume and material.

Given the shape of the optimal cantilevered branch with the furthest branch, we now ask if a direct comparison with the shapes of tree branches is possible. While the latter is influenced by multiple factors as discussed earlier, the measured shape of tree branches shows that the cross-sectional area of the branch, averaged over many trees, grows like $s^{3\pm0.26}$, where s is the distance from the branch tip [14]. Previous explanations for this were based on the notion of elastic similarity, *i.e.* the maximum stress (strain) at any location along the branch is the same [3], deduced using global considerations under the assumption of small deflection theory, for a given branch length. Here we see that the same result arises naturally as the unique local universal similarity solution (19) of our optimization problem near the tip. Our local explanation is attractive since it does not assume that the deflections are small, nor any information of the branch's global dimensions; indeed it suggests a simple way to maintain the shape of a growing branch using only local information. Of course, this local solution eventually must give way to a global shape that is determined by the shape and weight of the whole branch. Our optimal branch with the furthest reach assumes a very simple material law that ignores the microstructural complexity of wood in a branch which is also anisotropic and inhomogeneous, so that many questions about real branches remain. In particular, the introduction of additional fields such as the density ρ, modulus E and the material anisotropy also can be optimized; however this require further information of the restrictions on these fields that is currently unknown.

We conclude with a brief discussion of related optimization problems that out study also illuminates. When we relax the assumption of a solid cross-section an extreme departure is that of a thin circular tube, with a large bending stiffness (per unit mass of the branch); such a branch can therefore be much longer than one with a solid cross-section. The ultimate limit for the length of a thin circular tube is then determined by the condition that it does not buckle locally and form a kink-like structure (akin to a bent straw) under the influence of its own weight. Brazier [15] first described the onset of this ovalization and kinking instability which arises when the bending moment exceeds the critical value $2\sqrt{2}E\pi\hat{r}\hat{t}^2/(9\sqrt{1-\nu^2})$. For a tube of thickness $\hat{t}$ and radius $\hat{r}$ ($\hat{t} \ll \hat{r}$) the second moment of inertia is $I = \pi\hat{r}^3\hat{t}$, and the cross-sectional area is $\hat{a} = 2\pi\hat{r}\hat{t}$. Then, the constant dimensionless parameter that characterizes the geometry of all self-similar cross-sections $c = I/\hat{a}^2 = \hat{r}/(4\pi\hat{t})$ implies that the ratio $\hat{r}/\hat{t}$ must be fixed. Since the torque on the branch increases monotonically towards the base, as shown in fig. 2(c), to prevent Brazier buckling anywhere along the tubular branch, it is sufficient to prevent it from happening at the base. This is guaranteed via the inequality $cE\hat{a}^2\hat{\theta}_{\hat{s}} < 2\sqrt{2}E\pi\hat{r}\hat{t}^2/(9\sqrt{1-\nu^2})$ that sets a limit on c given by

$$c^{9/8}\left(\frac{\rho g}{\chi E}\right)^{3/8} V^{1/8} a^{1/2}\theta_s < \frac{1}{18\pi(1-\nu^2)}. \qquad (28)$$

As χ, a and θ are universal, eq. (28) immediately gives us a corresponding upper limit $\hat{r}/\hat{t}$ for given constants E, V and ν. Use the parameters above and a Poisson ratio $\nu = 0.5$, we find $\hat{r}/\hat{t} < 12.1$. For this critical ratio, the length of the neutral axis of the tapered tube is $L \approx 2.62(EV/\rho g)^{1/4}$ and the horizontal reach-out distance is $X \approx 2.20(EV/\rho g)^{1/4}$, which is significantly further than that for a solid circular cross-section. Similar calculations are possible for other cross-sections, although one must be careful to avoid bend-twist instabilities in elongated cross-sections, *i.e.* there are additional constraints on the geometric aspect ratio on the cross-section. It is also possible to allow the boundary conditions to vary as well —for example, if the clamping angle is a variable, it is intuitive that the reach can be extended still further— our preliminary calculations suggest that this is true. Clearly, including boundary, geometrical and material variations into the optimization of branch reach is a natural next step in this rich class of geometrically non-linear structural optimization problems.

* * *

We thank M. Venkadesan for discussions, A. Concha and the Wood lab for help with and access to the 3D printer, and the Harvard-NSF MRSEC for partial support.

REFERENCES

[1] Alexander R. M., *Optima for Animals* (Princeton University Press) 1996.
[2] Wolff J., *The Law of Bone Remodeling* (translation from the German) (Springer, New York) 1986.
[3] McMahon T., *Science*, **179** (1973) 1201.
[4] Nerdinger W., *Frei Otto, Complete Works: Lightweight Construction - Natural Design* (Birkhauser, Basel) 2005.
[5] Bendsoe M. and Sigmund O., *Topology Optimization* (Springer) 2004.
[6] Christensen P. W. and Klarbring A., *An Introduction to Structural Optimization* (Springer) 2008.
[7] Cherkaev A., *Variational Methods for Structural Optimization* (Springer) 2000.
[8] Keller J., *Arch. Ration. Mech. Anal.*, **5** (1960) 275.
[9] Keller J. and Niordsen F., *J. Math. Mech.*, **16** (1966) 433.
[10] Cox S. J., *Math. Intell.*, **14** (1992) 16.
[11] Farjoun Y. and Neu J., *Stud. Appl. Math.*, **115** (2005) 319.
[12] Horn H., *The Adaptive Geometry of Trees* (Princeton University Press) 1968.
[13] Love A. E. H., *A Treatise on the Mathematical Theory of Elasticity* (Dover Publications, New York) 1944.
[14] McMahon T. A. and Kronauer R. E., *J. Theor. Biol.*, **59** (1976) 443.
[15] Brazier L. G., *Proc. R. Soc. London, Ser. A*, **116** (1927) 773.